ISBN: 978-3-95450-227-1 ISSN: 2673-5490 doi:10.18429/JACoW-IPAC2022-TUPOMS036

COMMISSIONING OF THE LOWER EMITTANCE LATTICE AT SPEAR3*

K. Tian†, J. Corbett, S. Gierman, X. Huang, J. Kim, J. Langton, N. Parry, J. A. Safranek, J. J. Sebek, M. Song, Z. Zhang
SLAC National Accelerator Laboratory, Menlo Park, California, USA

Abstract

SPEAR3, commissioned in 2004, is a third-generation light source at the SLAC National Accelerator Laboratory. The low emittance lattice with an emittance of 10 nm had been operated for over a decade until the recent commissioning of a lower emittance lattice with the 7 nm emittance. The new lattice, with additional flexibility to adjust the sextupoles, has pushed toward the design limit of double-bend achromat lattice in SPEAR3. In this paper, we will elaborate on our commissioning experience for the new lattice in SPEAR3.

INTRODUCTION

By adopting a compact double-bend achromat (DBA) lattice design, SPEAR3 is efficient in achieving low emittance. However, with the growing number of next generation synchrotron radiation light sources under construction, there is a strong desire to push the limit of the lattice to lower emittance to benefit high brightness user experiments. Lower emittance lattice development efforts started in 2011. As a result, two lattice options, 6 nm lattice and 7 nm lattice, were developed [1]. Several hardware upgrades were identified to pave a pathway to user operation of the lower emittance lattice. First, the pulser of the second injection kicker, K2, was required to be upgraded to provide a stronger kick. This was completed in summer 2014. In the same year, new sextupole power supplies were added to break up the standard cell sextupoles from two large strings power supplies to eight smaller groups. The additional degrees of freedom allow simultaneous optimization of dynamic aperture and momentum aperture. The injection septum upgrade [2], which was completed in summer 2019, was essential to the operation of the lower emittance lattice. The new septum wall thickness was reduced from 5.4mm to 2.5 mm to provide efficient injection with the smaller dynamic aperture in the new lattice. The last hardware upgrade was the beam dump modification to address the radiation safety requirement. Following the installation of the beam dump in April 2021, SPEAR3 has started user beam operation in 7 nm lattice with highly reliable performance.

LATTICE OPTIONS

SPEAR3 has a race-track layout with 14 standard DBA cells and 4 matching DBA cells. The standard DBA cells need to be matched to the four matching cells of the two long straight sections. Based on the results of a global scan of the SPEAR3 standard DBA cell performance, it was determined to increase the horizontal tune by one unit to achieve emittance reduction. After explorations of the working point and phase advances of the matching cells, two lower emittance lattices were developed as upgrade options: 7 nm lattice and 6 nm lattice [1]. Selected parameters of these lattices, such as betatron tunes, emittance, effective emittance, horizontal/vertical beta functions at the ID straights, and the horizontal dispersion at the ID, are listed in Table 1. The parameters of the previous 10 nm lattice are listed for comparison.

Table 1: Lattice Parameters

	10 nm	**7 nm**	**6 nm**
ν_x, ν_y	14.106,6.177	15.10,6.16	15.32,6.18
ϵ_x (nm), w/IDs	9.6	6.7	6.1
$\epsilon_{x,eff}$ (nm)	10.1	7.2	6.7
$\beta_{x,ID}$ (m)	8.85	8.96	9.46
$\beta_{y,ID}$ (m)	4.86	5.29	5.24
$D_{x,ID}$ (m)	0.10	0.11	0.12

The lower emittance lattices boost the beam brightness significantly from the 10 nm lattice. Their effective emittances are 7.2 nm and 6.7 nm, respectively. Considering other factors such as the increased horizontal beta function in the 6 nm lattice, the two lattices offer comparable performance for most user experiments in SPEAR3. However, the 6 nm lattice is more challenging in terms of nonlinear beam dynamics, which is critical for efficient beam injection to the storage ring. Therefore, the 7 nm lattice was developed as the working option to serve as the initial operation lattice after the required hardware upgrades.

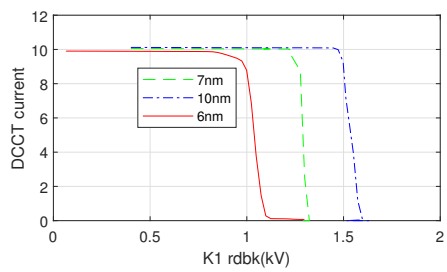

Figure 1: Dynamic aperture of different lattices.

During the development of the 7 nm and 6 nm lattices, various online optimization methods have been used to increase the dynamic aperture [3-5]. We believe that, after extensive nonlinear optimizations, we have explored the full potential of these two lattices. We compare the optimized dynamic

* Work supported by U.S. Department of Energy under Contract No. DE-AC02-76SF00515
† ktian@slac.stanford.edu

ISBN: 978-3-95450-227-1 ISSN: 2673-5490 doi:10.18429/JACoW-IPAC2022-TUPOMS036

aperture, measured by pulsing the K1 injection kicker for the 10 nm, 7 nm, and 6 nm lattices in Fig. 1. The dynamic aperture of the 7 nm lattice is adequate to deliver reliable injection performance identical to that from the 10 nm lattice for the user operations. However, the 6 nm lattice injection improvement is still ongoing.

3G DUMP MODIFICATION

For personnel radiation protection, SPEAR3 needs to control the electron beam loss points at adequately shielded areas. A preferred location to capture the electron beam loss is at the standard cell 3(3G) area, where a high nonlinear dispersion bump is deliberately introduced at the focusing quadrupole, 3G QFC. The vacuum chamber for the 3G QFC, built in 2003, had a welded insert serving as the beam dump by reducing the horizontal half aperture from the nominal 42mm to 30mm. The 3G dump had been sufficient for the 10 nm lattice to capture more than half of the lifetime beam loss and nearly all RF dump beam loss. However, tracking simulations show that this is no longer the case for the lower emittance lattices. With the 6 nm lattice, the septum is the main loss point for both types of beam loss. For the 7 nm lattice, the lifetime loss mostly occurs at the septum, but the RF dump loss distributes at different insertion devices depending on the magnet gap settings of the in vacuum insertion devices. Therefore, the operation of the lower emittance lattice of SPEAR3 required a modification to the horizontal aperture of the 3G dump. After numerical simulations, it was determined that the aperture of the 3G dump should be changed from -32mm to -15mm.

The new 3G dump, as shown in Fig. 2, is carefully designed for easy installation on top of the existing dump. This design provided us a cost effective solution without the need of building a new chamber and also enabled us to install the dump within a short period of time in early 2021.

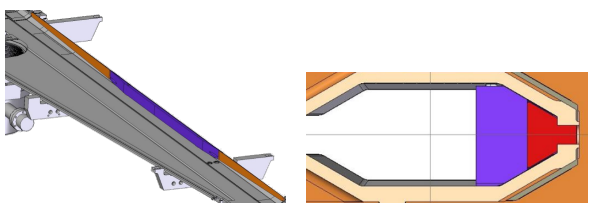

Figure 2: New SPEAR3 3G dump (purple) fitting on top the original dump(red).

Smooth transitions were included in the design of the new 3G dump to minimize the impedance effects. The longitudinal loss factors, k_l, of the new and original 3G dump were calculated using the time domain simulation code, T3P [6]. The results show that k_l of the new structure is -3.5mV/pC in comparison with -0.08mV/pC of the original 3G dump. Although this is a relatively significant increase over the previous impedance, it is still small. The estimated beam-induced heating to the dump from the normal operating SPEAR3 beam, 500mA beam in 280 bunches, is only about 2.4W. In addition, the transverse aperture of the 3G chamber reaches the minimum near the center of chamber and opens to the maximum at both ends. As a result, it is unlikely to trap RF modes in the structure. This is verified by the wake potential calculated up to 1 meter behind the bunch tail.

3G DUMP BEAM CHARACTERIZATION

The 7 nm lattice commissioning for user operations followed right after the installation of the new 3G dump. The major task during the commissioning was to conduct beam based measurements on the physical aperture of the new 3G dump to confirm it would be the primary loss point in the ring. Two different techniques were applied for the 3G dump aperture characterization, namely beam based aperture scan and RF beam loss measurement with a beam loss detector.

Aperture Scan

In a typical beam based aperture scan, a series of local orbit bumps with increasing amplitude was created using corrector magnets until the beam loss occurred at the physical aperture. At the 3G dump, the strength of the horizontal corrector magnets is insufficient to generate the required bump to probe the physical aperture. Instead, we first created a small amplitude DC bump at the 3G dump, then increased the amplitude of one of the injection kickers, K1, gradually until the beam was kicked out. Finally, we conducted tracking simulations for 200 turns to determine the loss point using the calculated beam orbits during the scan. In the tracking simulation, we set up the horizontal corrector magnets based on the actual closed orbit with the DC bump and K1 with the voltage corresponding to the beam loss and the calibration factor of 1.21 $mrad/kV$. One should note that the loss point can be either the 3G dump or the septum chamber because they are the limiting horizontal aperture in the ring, both in the -x direction. Therefore, we examined the turn by turn orbit at both locations in the tracking simulations. We conduced three scans with different DC bump magnitudes in 3G-QFC: dx=0 mm, -1 mm, and -3 mm, to ensure the beam would be lost at the 3G dump. The tracking results based on these scans are illustrated in Fig. 3. It appears that without an orbit bump, the beam was lost at the septum, which has the half aperture of 15mm in the -x direction. After adding the DC bump of -1mm or -3mm, the loss point changed from the septum to the 3G dump. The two scans indeed showed about 300 μm difference for the 3G dump aperture, which is reasonable when taking into account the possible discrepancies between the numerical calculations and the actual machine. More importantly, both results indicate that the as-built 3G dump aperture is smaller than 15mm, the expected value we would like to have.

Beam Loss Measurement

As described earlier, in the 7 nm lattice, when cutting off the storage ring RF power abruptly, according to the tracking studies, the beam loss will be captured mostly at the 3G dump if its physical aperture in the -x direction is less than 15mm. However, if a local orbit bump is applied to the

ISBN: 978-3-95450-227-1 ISSN: 2673-5490 doi:10.18429/JACoW-IPAC2022-TUPOMS036

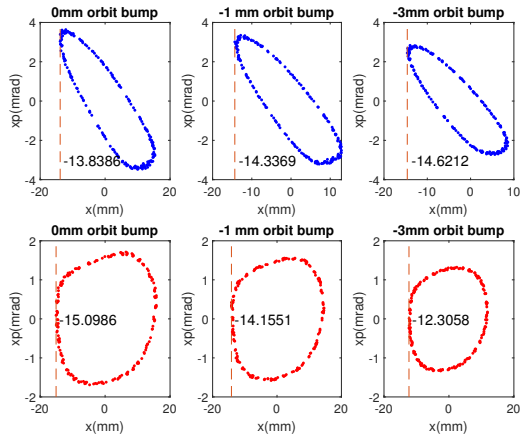

Figure 3: Tracking simulation results at the 3G dump (top row) and the septum(bottom row) for 3G dump aperture scan with different orbit bump.

beam orbit at the 3G dump in the +x direction, away from the dump, at some points, the RF dump loss can distribute to other locations. This process was simulated in tracking studies by changing the 3G dump aperture. Several Libera beam loss detectors(BLDs) and beam loss monitors(BLMs) [7] were acquired and installed in SPEAR3 before the start of the 7 nm lattice operational commission. One detector was installed at each location of the 3G dump and the septum. With these detectors, we were able to perform RF beam dump studies and compare with the tracking results. During the experiment, we filled a single bunch of 4mA in SPEAR3 with the 7 nm lattice loaded. The SPEAR3 RF was turned off abruptly with different DC bumps at the 3G dump, while the BLDs near the 3G dump and the septum were triggered to acquire the raw ADC data. The measurement data for the BLDs are compared in Fig. 4.

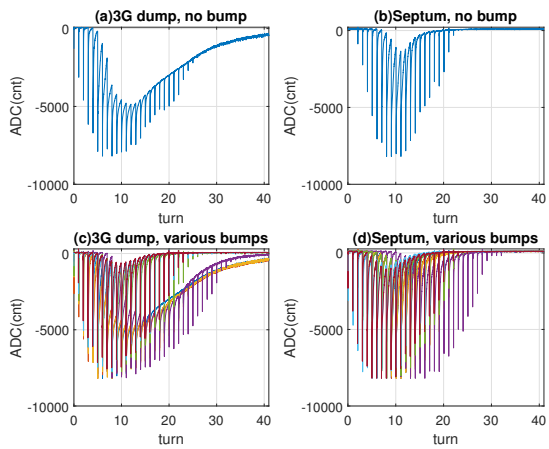

Figure 4: Raw ADC signals of the BLDs at 3G dump and Septum for the RF beam dump measurements

The Liberia BLD essentially is a photo multiplier tube (PMT) with a built-in scintillator to convert an individual loss event to a fast analog pulse lasting for about 20 ns. The ADC of the BLM samples this analog signal at a sampling rate up to $125 MHz$ or a sampling period of 8 ns. As a result, an isolated beam loss event should show up as a peak being formed by about 3 sampling points. However, due to the large number of electron lost when cutting off the RF, loss signals pile up and form broader peaks lasting nearly one turn as shown in Fig. 4. These broader peaks were seen in the BLD signals at the 3G dump and the septum. The lower envelope of the signals at the 3G dump appear to have larger amplitude and last longer when comparing the signal profiles in Fig. 4(a) and (b). This can suggest that the 3G dump has much higher loss event rates resulting more significant signal pile-up. Another observation from the BLD signals is that the beam appears to be gone completely within 30 turns after the RF is cut off. The results with different orbit bumps away from the 3G dump are shown in Fig. 4(c) and (d). They correspond to beam bumps of 0mm, 1.5mm, 2mm, 2.5mm, 3mm, 3.5mm, and 4mm, respectively, at the 3G dump. The signal profiles at the 3G dump change little when the beam bump is smaller than 3mm (green line).When the DC bump is larger than 3mm, the BLD signals have a reduced lower envelope and look similar to the signals from the septum BLD. We believe the integrals of the BLD signals in these measurements have strong correlations to the local beam loss rates, therefore we plot the results in Fig. 5 along with the tracking simulation results with different 3G dump apertures. If we correlate the turning points in the two plots, we conclude that the 3G dump aperture is about 14.25mm, which is consistent with results from the aperture scan.

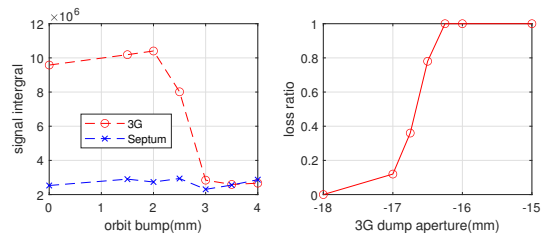

Figure 5: BLD measurments vs tracking simulations.

SUMMARY

After a multi-year effort, the 7 nm lattice for SPEAR3 was commissioned and delivered for user operation with reliable performance. The transition from the 10 nm lattice to the 7 nm lattice was smooth, thanks to the early beam dynamics and lattice optimization studies of the lattice. On the other hand, the 6 nm lattice still requires optimization in injection efficiency before delivering for user operations.

ACKNOWLEDGEMENTS

We would like to acknowledge T. Rabedeau for useful discussions. We want to thank the SPEAR3 operation and technical teams for supporting the work.

ISBN: 978-3-95450-227-1 ISSN: 2673-5490 doi:10.18429/JACoW-IPAC2022-TUPOMS036

REFERENCES

[1] X. Huang, Y. Nosochkov and J. Safranek, "Emittance upgrade for the SPEAR3 storage ring", *ICFA Beam Dynamics Newsletter*, vol. 71, pp. 266-280, 2017.

[2] M. A. G. Johansson, J. Langton, J. A. Safranek, and S. C. Gottschalk, "In-Vacuum Lambertson Septum for SPEAR3 Low Emittance Injection", in *Proc. IPAC'18*, Vancouver, Canada, Apr.-May 2018, pp. 3831–3834. doi:10.18429/JACoW-IPAC2018-THPAL078

[3] X. Huang and J. Safranek "Online optimization of storage ring nonlinear beam dynamics", *Phys. Rev. ST Accel. Beams*, vol. 18, issue 8, p. 084001, 2015. doi:10.1103/PhysRevSTAB.18.084001

[4] X. Huang and J. A. Safranek, "Beam-Based Optimization of Storage Ring Nonlinear Beam Dynamics", in *Proc. IPAC'17*, Copenhagen, Denmark, May 2017, pp. 3627–3630. doi:10.18429/JACoW-IPAC2017-THXA1

[5] Z. Zhang, M. Song and X. Huang, "Online accelerator optimization with a machine learning-based stochastic algorithm", *Mach. Learn.: Sci. Technol.*, vol. 2, p. 015014, 2021.

[6] O. Kononenko, L. Ge, C. Ko, Z. Li, C.-K. Ng, and L. Xiao, "Advances in Massively Parallel Electromagnetic Simulation Suite ACE3P", in *Proc. ICAP'15*, Shanghai, China, Oct. 2015, pp. 183–187. doi:10.18429/JACoW-ICAP2015-FRAJI3

[7] L. Torino and K. B. Scheidt, "New Beam Loss Detector System for EBS-ESRF", in *Proc. IBIC'18*, Shanghai, China, Sep. 2018, pp. 346–352. doi:10.18429/JACoW-IBIC2018-WEOB01